Direct Synthesis of Ordered Macroporous Silica Materials Functionalized with Polyoxometalate Clusters

Rick C. Schroden, Christopher F. Blanford, Brian J. Melde, Bret J. S. Johnson, and Andreas Stein*

Department of Chemistry, University of Minnesota, Minneapolis, Minnesota 55455

Received October 17, 2000. Revised Manuscript Received December 12, 2000

Three-dimensionally ordered macroporous (3DOM) silica materials functionalized with highly dispersed polyoxometalate clusters have been prepared via direct synthesis. Lacunary γ-decatungstosilicate clusters were incorporated into the wall structures of macroporous silica by reaction of the clusters in acidic solution with tetraethoxysilane, with or without addition of the polyfunctional linking group 1,2-bis(triethoxysilyl)ethane, followed by condensation around polystyrene colloidal crystals. Removal of the polystyrene template by extraction with a tetrahydrofuran/acetone solution produced the porous hybrid materials. The products were characterized by IR, solid-state ^{29}Si and ^{13}C NMR, scanning electron microscopy (SEM), transmission electron microscopy, X-ray energy-dispersive spectroscopy, and chemical analysis. The polyoxometalate clusters remained intact in the hybrid structures and were nearly molecularly dispersed throughout the walls of the 3DOM materials. High incorporation levels of cluster were obtained, with no bulk particles on the external surfaces. The materials were demonstrated to exhibit catalytic activity for the epoxidation of cyclooctene with an anhydrous H_2O_2/*t*-BuOH solution at room temperature.

Introduction

In recent years, the compositions of three-dimensionally ordered macroporous (3DOM) materials prepared by colloidal crystal templating have grown to include a large assortment of metal oxides, metals, alloys, polymers, and other compositions.[1−4] The interest in macroporous materials lies in their potential utility as catalyst supports,[5,6] separation materials,[7,8] battery materials,[9] thermal insulators,[10] and three-dimensional photonic crystals with optical band gaps.[11,12] Properties of 3DOM materials can be tailored by modifying their chemical composition and surface morphology. In the case of macroporous silicates, modifications have included organic functionalization[3,13] and dual templating to produce meso-/macroporous systems,[3,14−17] meso-/macroporous dye-functionalized silica,[18] and macroporous silicates with zeolitic microporous frameworks.[19−21]

In the current work, 3DOM silicates were modified by the incorporation of polyoxometalates (POMs) into the wall structures using a direct synthesis approach. The motivation for this work lies in the novel properties that POMs may introduce to the 3DOM materials.[22,23] The unique redox activities and high electron densities of POMs have led to their use as catalysts,[24,25] stains for electron microscopy,[26] and photo- and electrochromic materials.[27] Numerous investigations of POMs deposited on porous supports or entrapped in polymeric networks have been conducted, and these topics have

(1) Velev, O. D.; Jede, T. A.; Lobo, R. F.; Lenhoff, A. M. *Nature* **1997**, *389*, 447−448.
(2) Holland, B. T.; Blanford, C. F.; Stein, A. *Science* **1998**, *281*, 538−540.
(3) Holland, B. T.; Blanford, C. F.; Do, T.; Stein, A. *Chem. Mater.* **1999**, *11*, 795−805.
(4) Yan, H.; Blanford, C. F.; Smyrl, W. H.; Stein, A. *Chem. Commun.* **2000**, *16*, 1477−1478, and references therein.
(5) Diddams, P. *Inorganic Supports and Catalysts*; Smith, K., Ed.; Ellis Horwood: New York, 1992; pp 3−39.
(6) Johnson, B. J. S.; Stein, A. *Inorg. Chem.* **2001**, in press.
(7) Sarrade, S. J.; Rios, G. M.; Carles, M. *Sep. Purif. Technol.* **1998**, *14*, 19−25.
(8) Nakanishi, K.; Minakuchi, H.; Soga, N.; Tanaka, N. *J. Sol-Gel Sci. Technol.* **1998**, *13*, 163−169.
(9) Clough, T. J. U.S. Patent 5 895 732, 1999.
(10) Litovsky, E.; Shapiro, M.; Shavit, A. *J. Am. Ceram. Soc.* **1996**, *79*, 1366−1376.
(11) Wijnhoven, J. E. G. J.; Vos, W. L. *Science* **1998**, *281*, 802−804.
(12) Blanco, A.; Chomski, E.; Grabtchak, S.; Ibisate, M.; John, S.; Leonard, S. W.; Lopez, C.; Meseguer, F.; Miguez, H.; Mondia, J. P.; Ozin, G. A.; Toader, O.; van Driel, H. M. *Nature* **2000**, *405*, 437−440.
(13) Blanford, C. F.; Do, T. N.; Holland, B. T.; Stein, A. *Mater. Res. Soc. Symp. Proc.* **1999**, *549*, 61−66.
(14) Yang, P. D.; Deng, T.; Zhao, D. Y.; Feng, P. Y.; Pine, D.; Chmelka, B. F.; Whitesides, G. M.; Stucky, G. D. *Science* **1998**, *282*, 2244−2246.
(15) Antonietti, M.; Berton, B.; Göltner, C.; Hentze, H. P. *Adv. Mater.* **1998**, *10*, 154−159.
(16) Yin, J. S.; Wang, Z. L. *Appl. Phys. Lett.* **1999**, *74*, 2629−2631.
(17) Luo, Q.; Li, L.; Yang, B.; Zhao, D. Y. *Chem. Lett.* **2000**, 378−379.
(18) Lebeau, B.; Fowler, C. E.; Mann, S.; Farcet, C.; Charleux, B.; Sanchez, C. *J. Mater. Chem.* **2000**, *10*, 2105−2108.
(19) Holland, B. T.; Abrams, L.; Stein, A. *J. Am. Chem. Soc.* **1999**, *121*, 4308−4309.
(20) Huang, L. M.; Wang, Z. B.; Sun, J. Y.; Miao, L.; Li, Q. Z.; Yan, Y. S.; Zhao, D. Y. *J. Am. Chem. Soc.* **2000**, *122*, 3530−3531.
(21) Rhodes, K. H.; Davis, S. A.; Caruso, F.; Zhang, B.; Mann, S. *Chem. Mater.* **2000**, *12*, 2832−2834.
(22) Pope, M. T. *Heteropoly and Isopoly Oxometalates*; Springer-Verlag: Berlin, 1983.
(23) Pope, M. T.; Müller, A. *Angew. Chem., Int. Ed. Engl.* **1991**, *30*, 34−48.
(24) Mizuno, N.; Misono, M. *Chem. Rev.* **1998**, *98*, 199−218.
(25) Sadakane, M.; Steckhan, E. *Chem. Rev.* **1998**, *98*, 219−238.
(26) Keana, J. F.; Ogan, M. D.; Lu, Y.; Beer, M.; Varkey, J. *J. Am. Chem. Soc.* **1985**, *107*, 6714−6715.
(27) Yamase, T. *Chem. Rev.* **1998**, *98*, 307−326.

10.1021/cm000830b CCC: $20.00
Published on Web 01/24/2001

been recently reviewed.[24,25,27−31] In contrast, relatively few have involved the covalent incorporation of POMs into macromolecular hybrid materials.[32−38] A class of POM that is particularly attractive for the preparation of hybrid materials is the lacunary POM. Lacunary POMs, such as the mono- and divacant tungstosilicates $SiW_{11}O_{39}^{8-}$ and $SiW_{10}O_{36}$,$^{8-}$ are "unsaturated" Keggin ($SiW_{12}O_{40}^{4-}$) fragments.[22,39] Lacunary POMs have potential for forming hybrid materials due to nucleophilic surface oxygen atoms at the vacant site, which allow the covalent grafting of electrophilic groups, such as RSi^{3+}, RPO^{2+}, RSn^{3+}, RGe^{3+}, and RTi^{3+}.[22,31−34,38,40−50] In each case, the organic functionality is linked to the POM surface by E−O−W bridges (E = Si^{IV}, P^{V}, Sn^{IV}, Ge^{IV}, or Ti^{IV}), resulting in the saturation of the POM surface. Hybrid POM-based polymeric materials have been synthesized in this manner by functionalization of the lacunary POMs γ-$SiW_{10}O_{36}^{8-}$ and α-$SiW_{11}O_{39}^{8-}$ with reactive organic groups (vinyl, allyl, methacryl, and styryl), which were further polymerized with or without the presence of a cross-linking agent,[33,34,38] or by reaction of the clusters with bifunctional coupling molecules.[34]

The present study reports the preparation of 3DOM silica materials functionalized by polyoxometalates using direct synthesis procedures. The lacunary tungstosilicate cluster γ-$SiW_{10}O_{36}^{8-}$ was the POM chosen for these preparations because of its demonstrated reactivity toward siloxanes (Figure 1).[50] Two methods were explored. In the first, the γ-decatungstosilicate cluster was reacted with the bifunctional linking molecule 1,2-bis(triethoxysilyl)ethane (BTSE) under acidic conditions, followed by condensing with tetraethoxysilane (TEOS) in the presence of a polystyrene colloidal crystal template. In the second approach, TEOS was reacted directly with γ-decatungstosilicate under acidic conditions, followed by condensation around polystyrene colloidal crystals. The polystyrene template was subsequently removed from the materials by refluxing in a THF/acetone solution. The materials were characterized and structural features are described based on IR, solid-state MAS NMR, scanning electron microscopy (SEM), transmission electron microscopy (TEM), X-ray energy-dispersive spectroscopy (EDS), and chemical analysis. The direct syntheses produced ordered macroporous silica materials with high loadings of polyoxometalates incorporated nearly homogeneously throughout the wall structures. The materials formed by the two methods are described and compared. The method of template removal (by solvent extraction) was found to be important for retention of the POM unit and for incorporation of POMs within the wall structures. In contrast, the method of calcination for removal of the polystyrene template decomposed the POMs and produced large particles of a tungsten oxide species on the outside surface of the macroporous silicate. The catalytic activities of the POM-functionalized silica materials were tested for the epoxidation of cyclooctene and the results were compared to nonfunctionalized materials.

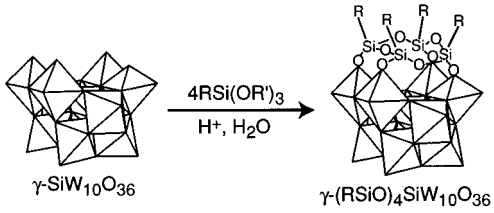

Figure 1. Reaction of organotrialkoxysilanes with the γ-decatungstosilicate cluster. Adapted from ref 50.

Experimental Section

Materials. Monodisperse polystyrene (PS) spheres were synthesized and packed into colloidal crystals by centrifugation as described previously.[2,3] PS spheres used in the syntheses had diameters of 297 ± 5 nm (for **POM-SiO$_2$A**) and 330 ± 10 nm (for **POM-SiO$_2$B**). Macroporous silica (**3DOM SiO$_2$**) was prepared according to literature methods.[2,3] All macroporous samples had amorphous silica walls, which results in a broad distribution of mesoporosity and surface areas ranging from 150 to 250 m^2/g.[3] The preparation of $K_8[\gamma\text{-}SiW_{10}O_{36}]\cdot 12H_2O$ (γ-$SiW_{10}O_{36}$) has been described previously.[39] Reagents were obtained from the following sources: tetraethoxysilane (TEOS), tetrahydrofuran (THF), HCl (37%), *cis*-cyclooctene, and manganese dioxide were from Aldrich; absolute ethanol was from Aaper Alcohol and Chemical Co.; acetone was from Pharmco Products Inc.; 1,2-bis(triethoxysilyl)ethane (BTSE) was from Gelest; H_2O_2 (30% aqueous solution), *tert*-butanol, and anhydrous magnesium sulfate were from Mallinckrodt. All chemicals were used as received without further purification. Water used in all syntheses was distilled and deionized to 17.7 MΩ-cm.

Synthesis of POM-SiO$_2$A. γ-Decatungstosilicate cluster-functionalized 3DOM materials containing bis(silyl)ethane-linking molecules were synthesized from mixtures of typical molar composition 53.2:4.00:1.00:660:203:22.9 TEOS:BTSE: $K_8[\gamma\text{-}SiW_{10}O_{36}]\cdot 12H_2O$:$H_2O$:ethanol:HCl (Figure 2A). γ-$SiW_{10}O_{36}$ was stirred with H_2O in a small vial at room temperature. BTSE, ethanol, and HCl were thoroughly mixed in a separate container and then added to the γ-$SiW_{10}O_{36}$ mixture with vigorous stirring. The pH of the resulting solution was ≈1. The solution turned clear yellow after a few minutes of stirring. The solution was covered and stirred for 4 h at room temperature. TEOS was added to the vial, and the sample was stirred for 3 min. The solution was then applied dropwise to completely cover millimeter-thick layers of dried PS sphere col-

(28) Kozhevnikov, I. V. *Chem. Rev.* **1998**, *98*, 171−198.
(29) Coronado, E.; Gómez-García, C. J. *Chem. Rev.* **1998**, *98*, 273−296.
(30) Klemperer, W. G.; Wall, C. G. *Chem. Rev.* **1998**, *98*, 297−306.
(31) Katsoulis, D. E. *Chem. Rev.* **1998**, *98*, 359−387.
(32) Knoth, W. H. *J. Am. Chem. Soc.* **1979**, *101*, 2211−2213.
(33) Judeinstein, P. *Chem. Mater.* **1992**, *4*, 4−7.
(34) Judeinstein, P. *J. Sol-Gel. Sci. Technol.* **1994**, *2*, 147−151.
(35) Stein, A.; Fendorf, M.; Jarvie, T. P.; Mueller, K. T.; Benesi, A. J.; Mallouk, T. E. *Chem. Mater.* **1995**, *7*, 304−313.
(36) Holland, B. T.; Isbester, P. K.; Blanford, C. F.; Munson, E. J.; Stein, A. *J. Am. Chem. Soc.* **1997**, *119*, 6796−6803.
(37) Holland, B. T.; Isbester, P. K.; Munson, E. J.; Stein, A. *Mater. Res. Bull.* **1999**, *34*, 471−482.
(38) Mayer, C. R.; Thouvenot, R.; Lalot, T. *Chem. Mater.* **2000**, *12*, 257−260.
(39) Tézé, A.; Hervé, G. *Inorg. Synth.* **1990**, *27*, 85−96.
(40) Knoth, W. H. *J. Am. Chem. Soc.* **1979**, *101*, 759−760.
(41) Judeinstein, P.; Deprun, C.; Nadjo, L. *J. Chem. Soc., Dalton Trans.* **1991**, 1991−1997.
(42) Kim, G.; Hagen, K. S.; Hill, C. L. *Inorg. Chem.* **1992**, *31*, 5316−5324.
(43) Xin, F.; Pope, M. T.; Long, G. J.; Russo, U. *Inorg. Chem.* **1996**, *35*, 1207−1213.
(44) Xin, F.; Pope, M. T. *Inorg. Chem.* **1996**, *35*, 5693−5695.
(45) Judeinstein, P.; Sanchez, C. *J. Mater. Chem.* **1996**, *6*, 511−525.
(46) Mayer, C. R.; Thouvenot, R. *J. Chem. Soc., Dalton Trans.* **1998**, 7−13.
(47) Gouzerh, P.; Proust, A. *Chem. Rev.* **1998**, *98*, 77−111.
(48) Mayer, C. R.; Herson, P.; Thouvenot, R. *Inorg. Chem.* **1999**, *38*, 6152−6158.
(49) Ribot, F.; Sanchez, C. *Comments Inorg. Chem.* **1999**, *20*, 327−371.
(50) Mayer, C. R.; Fournier, I.; Thouvenot, R. *Chem. Eur. J.* **2000**, *6*, 105−110.

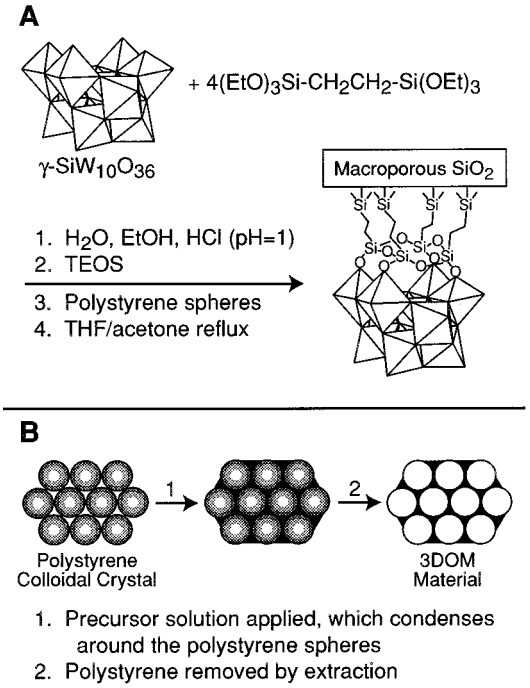

Figure 2. (A) Synthesis of **POM-SiO$_2$A**. (B) Structural control of **POM-SiO$_2$** materials by polystyrene colloidal crystal templating.

loidal crystals, which were crushed and deposited on filter paper in a Büchner funnel with suction applied (Figure 2B). The composite sample was allowed to dry in air at room temperature for 24 h. PS was removed from the sample by extraction for 5 days in a refluxing solution of 1:1 (v/v) THF and acetone. The white powder product was recovered by filtration and washed with THF/acetone and then acetone. The mean macropore size was 234 ± 10 nm.

Typical analysis (wt %) for **POM-SiO$_2$A**: 22% Si, 22% W, 8% C. Calculated for **POM-SiO$_2$A**: 1.2 wt % C from organosilane (BTSE) based on synthesis gel ratio and Si analysis; 1.6% of the Si is from γ-$SiW_{10}O_{36}$ (based on synthesis gel ratio), 1.5% (based on Si and W analysis). The majority of the excess carbon in **POM-SiO$_2$A** was due to incomplete removal of the polystyrene template. Approximately 99% of the polystyrene was removed by the solvent extraction process. Washing the samples with water did not change the W loading.

Synthesis of POM-SiO$_2$B. γ-Decatungstosilicate cluster-functionalized 3DOM silica materials (without bis(silyl)ethane linkers) were prepared from mixtures of typical molar composition 33.3:1.00:413:127:14.4 TEOS:$K_8[\gamma$-$SiW_{10}O_{36}]\cdot 12H_2O$:$H_2O$:ethanol:HCl. γ-$SiW_{10}O_{36}$ was stirred with H_2O in a small vial at room temperature. TEOS, ethanol, and HCl were thoroughly mixed in a separate container and then added to the γ-$SiW_{10}O_{36}$ mixture with vigorous stirring. The pH of the resulting solution was ≈1. The sample was stirred for 3 min. The solution was then applied to PS spheres and extracted with THF/acetone as described above. The mean macropore size was 265 ± 10 nm. As an alternative template removal technique, the as-synthesized sample was calcined in air at 500 °C for 5 h. This treatment decomposed the polyoxometalate clusters, producing a bulk tungsten oxide species on the surface of the macroporous material. All further references to **POM-SiO$_2$B** apply to the solvent-extracted material, unless specifically stated otherwise.

Typical analysis (wt %) for **POM-SiO$_2$B**: 17% Si, 28% W, 7% C. Calculated for **POM-SiO$_2$B**: 2.9% of the Si is from γ-$SiW_{10}O_{36}$ (based on synthesis gel ratio), 2.5% (based on Si and W analysis). All of the C in **POM-SiO$_2$B** was due to incomplete removal of the polystyrene template. Approximately 99% of the polystyrene was removed by the solvent extraction process. Washing the samples with water did not change the W loading.

Characterization. Infrared spectroscopy was performed on a Nicolet Magna-IR 760 spectrometer with mid-IR and far-IR capability. Spectra were obtained using the powdered samples in FT-IR grade KBr pellets for the mid-IR range and spectrophotometric grade polyethylene pellets for the far-IR range. Solid-state NMR spectra were obtained on a Chemagnetics CMX-400 Infinity spectrometer at room temperature with a 7.5-mm zirconia rotor spinning at 4 kHz. ^{13}C CP MAS NMR experiments (100.63 MHz, 4-μs ^{1}H 90° pulse width, 2-s pulse delay) used a hexamethylbenzene standard. ^{1}H-^{29}Si CP MAS NMR spectra (79.49 MHz, 3.5-μs ^{1}H 90° pulse width, 4-s pulse delay) used a PDMS standard, and ^{29}Si MAS NMR, single-pulse, spectra (79.49 MHz, 3-μs pulse width, 40-s pulse delay) used a tetramethylsilane standard. Scanning electron micrographs (SEM) were obtained on a Hitachi S-800 scanning electron microscope operating at 4 kV. Samples for SEM were dusted on an adhesive conductive carbon disk attached to an aluminum mount. X-ray energy-dispersive spectra (EDS) were acquired using an Oxford Link eXL X-ray energy-dispersive spectrometer. Transmission electron micrographs (TEM) were obtained on a Philips CM30 transmission electron microscope operating at 300 kV with a LaB_6 filament. Samples for TEM were prepared by sonicating the powder in absolute ethanol for 30 min and then depositing five drops of the suspension on a holey carbon film. Images were recorded on a slow-scan CCD camera. EDS spectra were recorded on an EDAX PV9900. Multiple spectra were acquired, and the ratios between peak intensities did not vary significantly between samples. The Cu signals in the spectra are from the specimen support grid. Elemental analyses were performed for Si and W at the Geochemical Lab, University of Minnesota, Minneapolis, MN, and for C at Atlantic Microlab Inc., Norcross, GA. Gas chromatography (GC) was performed on a Hewlett-Packard 5890A gas chromatograph (oven temperature 80 °C, injector temperature 100 °C, detector temperature 200 °C, He carrier gas, 5 mL/min flow rate), with an FID detector and a J & W Scientific DB-5 column (film thickness 1.5 μm, length 15 m, inner diameter 0.53 mm).

Catalytic Testing. The **POM-SiO$_2$A** and **POM-SiO$_2$B** materials were tested for catalytic activity in the epoxidation of cyclooctene with anhydrous H_2O_2/*t*-BuOH at room temperature according to literature methods,[51] and the results were compared to an experiment with a **3DOM SiO$_2$** catalyst and a blank experiment. Anhydrous H_2O_2/*t*-BuOH was prepared by mixing 200 mL of *t*-BuOH and 60 mL of H_2O_2 (30% aqueous solution) with excess anhydrous $MgSO_4$.[51] Catalytic tests were performed by stirring the catalyst (130 mg) in a flask with anhydrous H_2O_2/*t*-BuOH (8 mL) and *cis*-cyclooctene (0.5 mL) for 24 h. Samples were then filtered to remove the catalyst and quenched with MnO_2. The products and reaction progress were monitored by GC.

Results and Discussion

Product Characterization. *IR Spectra*. The IR spectra of the as-synthesized **POM-SiO$_2$** materials are dominated by PS absorptions. The PS template was extracted in refluxing THF/acetone, and its removal was monitored by IR. After 5 days most of the PS was removed, with the majority of the PS features absent from the spectra of the extracted materials. The most intense PS bands did not disappear completely, indicating that some PS remained in the **POM-SiO$_2$** materials. However, these bands were significantly reduced in intensity.

The γ-decatungstosilicate cluster displays a characteristic infrared fingerprint in the region from ca. 1000 to 300 cm^{-1}.[39] The cluster fingerprint is partially obscured in the **POM-SiO$_2$** materials because of the

(51) Briot, E.; Piquemal, J.; Vennat, M.; Brégeault, J.; Chottard, G.; Manoli, J. *J. Mater. Chem.* **2000**, *10*, 953−958.

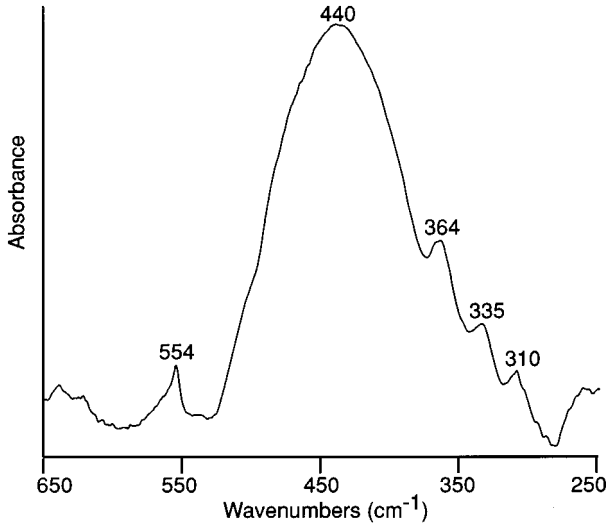

Figure 3. Far-IR spectrum of **POM-SiO$_2$A**.

presence of strong IR bands from the silica framework. Intense and broad stretching vibrations at ca. 1100 cm^{-1} ν_{asym}(Si−O−Si), 950 cm^{-1} ν(Si−OH), and 800 cm^{-1} ν_{sym}(Si−O−Si), and bending vibration at 440 cm^{-1} δ(Si−O−Si) are observed for the **POM-SiO$_2$** materials because of the silica framework.[52] These silica bands hinder characterization of the polyoxometalate species in the mid-IR region of the spectra. The far-IR region, however, contains peaks specific to the nature of the polyoxometalate species that allow identification of the cluster in the hybrid materials. Relevant bands for the $K_8[\gamma\text{-}SiW_{10}O_{36}]\cdot 12H_2O$ cluster precursor in the far-IR region are observed at 556 cm^{-1} δ_{asym}(Si−O) and 359, 318, and 306 cm^{-1} δ_{asym}(W−O−W).[39] **POM-SiO$_2$A** displays IR bands at 554 cm^{-1} δ_{asym}(Si−O) and 364, 335, and 310 cm^{-1} δ_{asym}(W−O−W) (Figure 3). **POM-SiO$_2$B** displays similar bands at 555 cm^{-1} δ_{asym}(Si−O) and 365, 333, and 309 cm^{-1} δ_{asym}(W−O−W). The presence of absorptions for δ_{asym}(Si−O) characteristic of γ-$SiW_{10}O_{36}$ in the **POM-SiO$_2$** materials confirms retention of the polyoxometalate structure in the hybrid materials. The shifting of δ_{asym}(W−O−W) bands to higher frequencies, compared to the cluster precursor, is attributed to saturation of the polyoxometalate moiety through the fixation of siloxane units. Similar shifts have been observed upon functionalization of the γ-$SiW_{10}O_{36}$ polyoxometalate by grafting molecular species.[38,48,50] The IR results suggest that the structural integrity of the polyoxometalates has been preserved and the clusters are chemically bound to the hybrid 3DOM materials. Further confirmation of the nature of POM species present in the materials is provided by ^{29}Si MAS NMR experiments (see below).

As an alternative template removal technique, the as-synthesized **POM-SiO$_2$B** materials were calcined in air at 500 °C for 5 h. This technique completely removed the polystyrene from the structure (IR); however, it also appears to have decomposed the polyoxometalate clusters to an unidentified tungsten oxide species. The IR spectrum of the calcined material displays bands at 362, 338, 330, and 299 cm^{-1}, which are likely due to tungsten−oxygen deformations. No band was observed for the δ_{asym}(Si−O) stretch characteristic of γ-$SiW_{10}O_{36}$, which indicates decomposition of the POM clusters.

Solid-State NMR. To confirm incorporation and connection of the POMs with the 3DOM silica framework, the **POM-SiO$_2$** materials were analyzed by solid-state ^{29}Si MAS NMR. The γ-decatungstosilicate cluster displays a characteristic peak at −85.2 ppm due to the central Si(OW)$_4$ unit. The ^{29}Si MAS NMR spectra of the **POM-SiO$_2$** materials are given in Figure 4. Peak positions (ppm) and their respective assignments for **POM-SiO$_2$A** are as follows: −110.6, Q^4 (Si*(OSi)$_4$); −100.9, Q^3 (Si*(OSi)$_3$(OH)); −91.1, Q^2 (Si*(OSi)$_2$(OH)$_2$); −86.4, central SiO_4 of cluster; broad feature from −44 to −68, T^n (Si*(R)(OSi)$_n$(OH)$_{3-n}$). Peak positions (ppm) and assignments for **POM-SiO$_2$B** are as follows: −110.5, Q;[4] −100.8, Q^3; −91.1, Q^2; −84.5, central SiO_4 of cluster. The appearance of cluster Si peaks in the spectra indicates incorporation of the POMs into the materials. The presence of Q^2 and Q^3 peaks in the ^{29}Si NMR spectra of the **POM-SiO$_2$** materials is indicative of surface silanol groups and incomplete condensation of the silica frameworks (**POM-SiO$_2$A** integrated areas of Q peaks: 8% Q^2, 50% Q^3, 42% Q;[4] **POM-SiO$_2$B**: 8% Q^2, 49% Q^3, 43% Q^4). These results, however, are typical for solvent-extracted 3DOM silicates. The series of T^n peaks in the ^{29}Si NMR spectra of **POM-SiO$_2$A** arise from the organosiloxane linker. The T^n peaks are only slightly resolved, with approximate peak positions for T^1, T^2, and T^3 (based on deconvolution) at −46, −55, and −64 ppm, respectively. Incorporation of the organosiloxane units into the structure of **POM-SiO$_2$A** was also confirmed by ^{13}C CP MAS NMR, with a strong resonance present at 5 ppm, which was attributed to the Si−CH_2CH_2−Si group.

The nature of the cluster species present in the macroporous silica frameworks can be determined by comparison of the results for the single-pulse and ^{1}H-^{29}Si cross-polarization (CP) NMR spectra. In the CP experiment, the intensities of the Si peaks are enhanced by polarization transfer from the abundant ^{1}H nuclei to the rare ^{29}Si nuclei, provided that the silicon nuclei are near protons.[53] This results in a considerable improvement in the signal-to-noise (S/N) ratio of the ^{29}Si NMR spectra and selective enhancement of the signals for Si nuclei with nearby protons (e.g., silicon atoms in a T^n or Q^{1-3}, but not in a Q^4 environment).[53] The single-pulse ^{29}Si MAS NMR spectrum of **POM-SiO$_2$A** (Figure 4A) has a small shoulder in the expected position of the cluster Si. The low quantity of cluster Si compared to structural Si of the silica framework is responsible for the low intensity of the peak. The cluster peak is clearly observed in the CP spectrum (Figure 4B). The presence of this peak confirms retention of the POM cluster in the hybrid macroporous material. The shift in position of the peak from the parent cluster is consistent with the grafting of organosiloxane units onto the POM surface.[50] The clearly defined central Si cluster peak in the CP spectrum of **POM-SiO$_2$A**, compared to its single-pulse spectrum, may be due in part to the overall higher S/N observed for the CP experiment. In addition, the more intense POM central Si peak in the CP spectrum

(52) Brinker, C. J.; Scherer, G. W. *Sol−Gel Science: the Physics and Chemistry of Sol−Gel Processing*; Academic Press: San Diego, 1990.

(53) Engelhardt, G.; Michel, D. *High-Resolution Solid-State NMR of Silicates and Zeolites*; Wiley: Norwich, 1987.

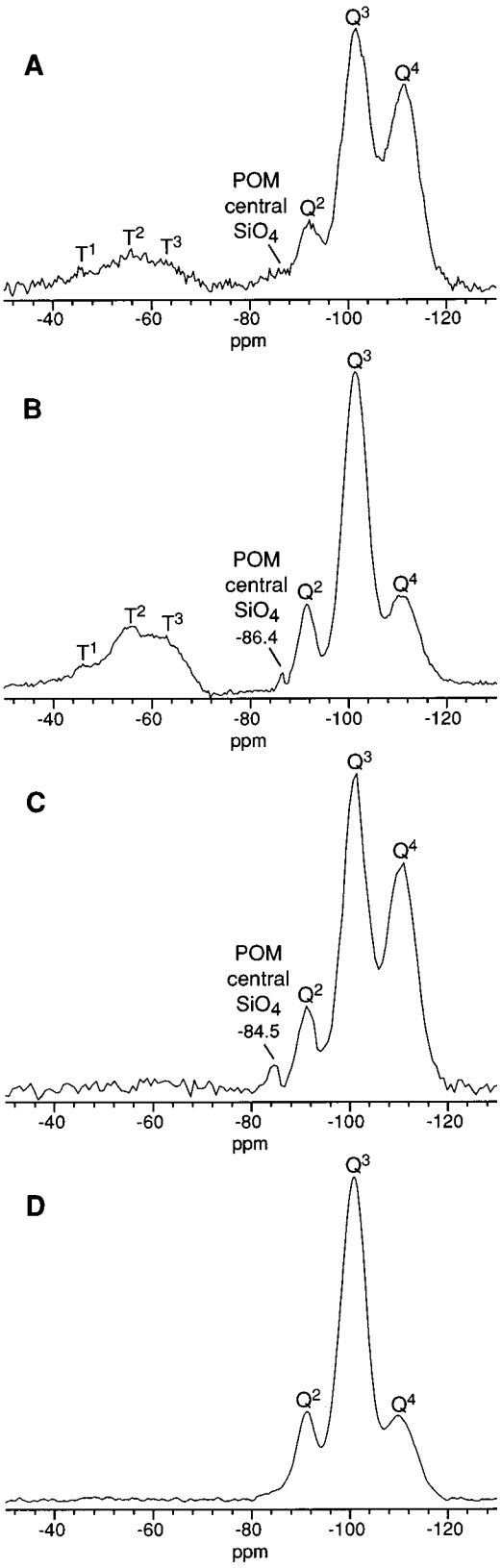

Figure 4. ^{29}Si MAS NMR: (A) **POM-SiO$_2$A** (single pulse), (B) **POM-SiO$_2$A** (^{1}H-^{29}Si CP), (C) **POM-SiO$_2$B** (single pulse), and (D) **POM-SiO$_2$B** (^{1}H-^{29}Si CP).

is likely due to grafted organosiloxane groups, which have protons present in the organic groups that are close enough to transfer magnetization and enhance this signal in the CP experiment. This notion is supported by the ^{29}Si NMR results for the **POM-SiO$_2$B** sample (which does not contain organosiloxane units). The single-pulse ^{29}Si MAS NMR spectrum of **POM-SiO$_2$B** (Figure 4C) exhibits a peak at −84.5 ppm, which has been assigned to the central SiO_4 unit of the POM cluster. The clearly defined cluster peak in this sample was attributed to the higher fraction of cluster Si in the **POM-SiO$_2$B** material compared to that in **POM-SiO$_2$A**. This peak is not present in the corresponding CP spectrum (Figure 4D), as expected because of the absence of protons near the cluster Si. Repeated experiments and NMR analysis have produced the same results. The presence of cluster peaks in the ^{29}Si MAS NMR spectra of the **POM-SiO$_2$** materials confirms retention of the POM in the hybrid materials. The shifts in peak positions of the cluster Si and the contrasting results observed for **POM-SiO$_2$A** and **POM-SiO$_2$B** in the ^{29}Si MAS NMR experiments suggest that different modes of linking have occurred, with the polyoxometalate clusters in **POM-SiO$_2$A** attached to the silica framework through organosiloxane linkages.

SEM and EDS. Scanning electron microscopy (SEM) was used to assess the order of the **POM-SiO$_2$** materials and to provide a preliminary determination of the homogeneity of the POM species throughout the silica framework. An examination of both the secondary electron (SE) and backscattered electron (BSE) images of the materials allows determination of whether the POMs are incorporated into the 3DOM silica structures. BSEs respond to composition, local specimen inclination and topology, crystallography, and internal magnetic fields.[54] Composition is the most important factor in the qualitative assessment of this material by BSE imaging. The ratio of the number of BSEs to electrons incident on the sample from the beam is called the BSE coefficient or η. The relationship between η and atomic number, Z, has been fit empirically.[55] For atomically homogeneous mixtures, η follows a simple rule of mixtures based on the relative mass concentrations of each species.[56] Tungsten(VI) oxide has an average BSE coefficient of 0.40, while $\eta_{avg} = 0.38$ for γ-$SiW_{10}O_{36}$ and $\eta_{avg} = 0.13$ for SiO_2. Therefore, areas that have POM clusters or decomposition products thereof separate from the 3DOM silica structure appear approximately 3 times brighter in the BSE images. This effect is demonstrated by the SEM images of a sample of **POM-SiO$_2$B** that has been calcined to remove the polystyrene template (Figure 5A−D). The left images (Figure 5A,C) are low- and high-magnification SE images, and the right images (Figure 5B,D) are BSE images for the corresponding areas of the sample. A bulk crystalline species is observed protruding from the surface of the sample. These crystalline domains are observed by their topology in the SE images. The BSE images show that they are probably tungsten-rich because they appear significantly brighter than the surrounding silica matrix. These domains are likely a tungsten(VI) oxide species

(54) Goldstein, J. I.; Newbury, D. E.; Echlin, P.; Joy, D. C.; Romig, A. D., Jr.; Lyman, C. E.; Fiori, C.; Lifshin, E. *Scanning Electron Microscopy and X-ray Microanalysis: A Text for Biologists, Materials Scientists, and Geologists*; 2nd ed.; Plenum Press: New York, 1992.

(55) Reuter, W. *Ionization function and its application to the electron probe analysis of thin films*; Shinoda, G., Kohra, K., Ichinokawa, T., Eds.; University of Tokyo Press: Tokyo, 1972; pp 121−130.

(56) Heinrich, K. F. J. *Electron probe microanalysis by specimen current measurement*; Castaing, R., Deschamps, P., Philibert, J., Eds.; Hermann: Paris, 1966; pp 159−167.

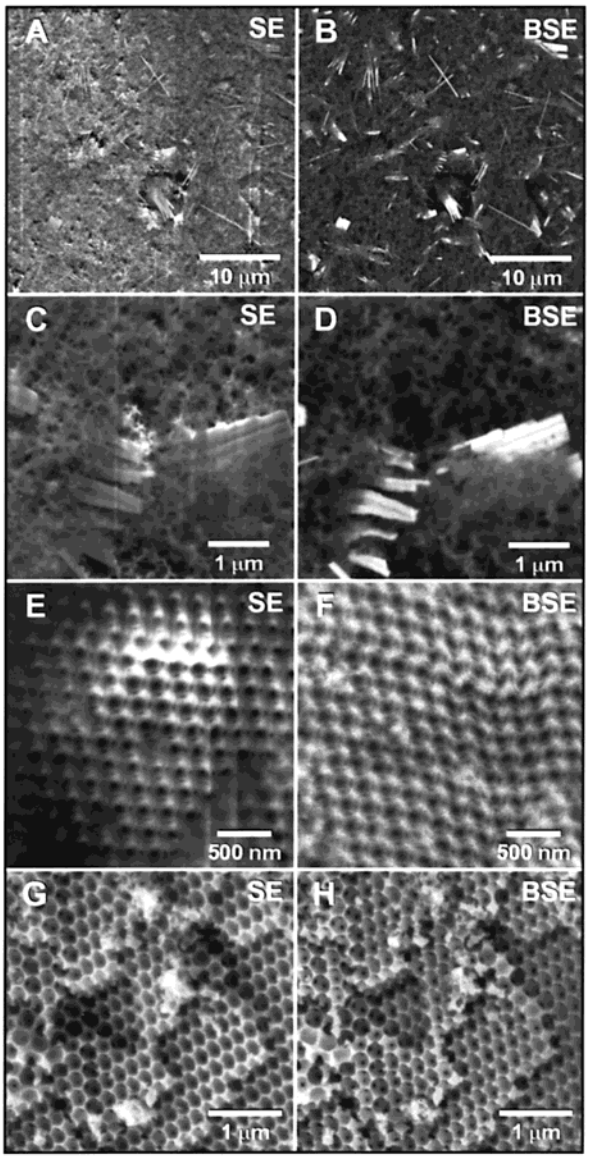

Figure 5. SEM: (A) calcined **POM-SiO$_2$B** (low-magnification SE image), (B) calcined **POM-SiO$_2$B** (low-magnification BSE image), (C) calcined **POM-SiO$_2$B** (high-magnification SE image), (D) calcined **POM-SiO$_2$B** (high-magnification BSE image), (E) **POM-SiO$_2$A** (SE), (F) **POM-SiO$_2$A** (BSE), (G) **POM-SiO$_2$B** (SE), and (H) **POM-SiO$_2$B** (BSE).

formed from the thermal decomposition of the polyoxometalates.

SEM analysis of the solvent-extracted **POM-SiO$_2$A** (Figure 5E,F) and **POM-SiO$_2$B** (Figure 5G,H) materials showed no distinct cluster or tungsten oxide aggregates in the SE or BSE images. The X-ray energy-dispersive spectra (EDS) of these materials showed the presence of tungsten in the sample; therefore, the size of any tungstate species in the materials must be below the spatial resolution of the SEM. The absence of bright regions in the BSE images indicates that the POMs are highly dispersed throughout the structure.

TEM and EDS. The **POM-SiO$_2$** materials were also examined by transmission electron microscopy (TEM). The particles of **POM-SiO$_2$A** were extremely well ordered (as evidenced by the image in Figure 6A). The TEM image in Figure 6A shows the microstructure of **POM-SiO$_2$A**. The walls appear as the dark, skeletal

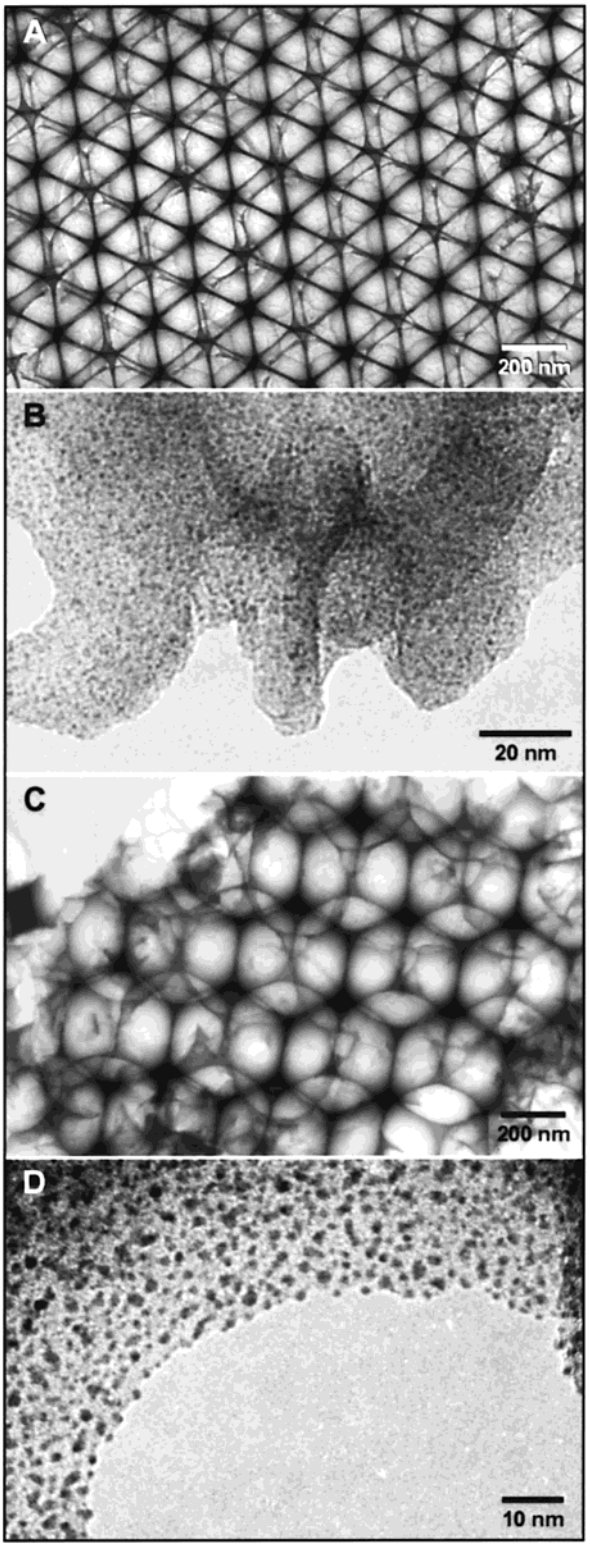

Figure 6. TEM images showing (A) ordered porous structure of **POM-SiO$_2$A**, (B) POM clusters (which appear as dark spots) highly dispersed on a thin section of the framework of **POM-SiO$_2$A**, (C) ordered porous structure of **POM-SiO$_2$B**, and (D) POM clusters highly dispersed on a thin section of the framework of **POM-SiO$_2$B**.

structure. The image in Figure 6B is a close-up of the wall structure, showing the high molecular weight clusters, which appear as 1−2-nm dark spots on the thin section of wall. During the sample's exposure to the electron beam during analysis, the dark spots associated

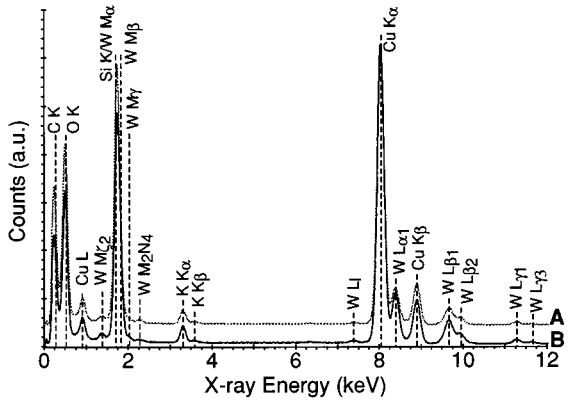

Figure 7. X-ray energy-dispersive spectra (EDS) taken in the TEM of (A) **POM-SiO$_2$A** and (B) **POM-SiO$_2$B**.

with incorporated cluster species grew visibly. At the start of the analysis, the dark spots were nearly indistinguishable from the amorphous silica background. After a few minutes of exposure to the electron beam, the clusters grew to the size that they appear in the image in Figure 6B and then stopped expanding. Therefore, the initial size of this species is probably less than 2 nm, suggesting a nearly molecular dispersion of POM clusters throughout the silica framework, given the size of a POM cluster is ca. 1 nm.

TEM analysis of **POM-SiO$_2$B** showed similar features (Figure 6C,D), although the silica framework possessed less long-range order. The high-magnification image (Figure 6D) also clearly showed a high loading of clusters dispersed throughout the structure. The EDS spectra of the **POM-SiO$_2$** materials are given in Figure 7. These spectra showed the presence of tungsten in the materials, indicating that the POMs have been incorporated into the silica frameworks. The Cu signals arise from the sample holder.

Structure and Composition. Characterization of the **POM-SiO$_2$** materials indicated that the syntheses produced three-dimensionally ordered macroporous materials with high loadings of highly dispersed polyoxometalates covalently incorporated within the wall structures. IR and solid-state ^{29}Si MAS NMR of the **POM-SiO$_2$** materials confirmed that the polyoxometalates remained intact in the hybrid macroporous silica materials. Both **POM-SiO$_2$A** and **POM-SiO$_2$B** exhibited IR and ^{29}Si NMR peaks that were characteristic of the central $Si(OW)_4$ unit of the γ-$SiW_{10}O_{36}$ POM. The shifts to higher frequency, as compared with the starting POM, of the cluster bands in the IR spectra can be attributed to saturation of the POM moieties through grafting of siloxane units and, therefore, linking to the silicate structure. The opposite shifts in position of the cluster Si peak in the ^{29}Si NMR spectra of **POM-SiO$_2$A** vs **POM-SiO$_2$B** are consistent with different modes of POM linking. In the **POM-SiO$_2$A** material, γ-$SiW_{10}O_{36}$ was pre-reacted with the bifunctional bis(silyl)ethane group prior to condensation with the silica network. The organic groups provided a method of linking the clusters to the silicate structure. In the case of **POM-SiO$_2$B**, the lacunary POM cluster was condensed directly with the silica structure. The different methods of cluster linking in the two materials was confirmed by the single-pulse and CP ^{29}Si MAS NMR techniques, which indicated that the clusters in **POM-SiO$_2$A** were likely linked to the silica framework by bis(silyl)ethane groups, whereas the clusters in **POM-SiO$_2$B** condensed directly with the silica matrix.

Table 1. Catalysis Results for the Epoxidation of Cyclooctene with Anhydrous H_2O_2/*t*-BuOH over Various Catalysts[a]

catalyst	W content (wt %)	cyclooctene conversion (%)
POM-SiO$_2$A	22	11
POM-SiO$_2$B	28	24
3DOM SiO$_2$	0	0
blank	0	0

[a] Conversion is based on substrate. Selectivity is 100% for the epoxide.

As a further test of linking of the clusters to the silicate framework, the **POM-SiO$_2$** materials were washed with large amounts of water. Unlike other systems in which POMs have been supported on porous solids using impregnation techniques,[57] washing with water did not result in the leaching of POMs from the solids. Tungsten loading (elemental analysis) and IR spectra of washed samples remained the same.

Elemental analysis of the **POM-SiO$_2$** materials showed that, while the molar concentration of POMs was relatively low, the weight percentage of POMs was very high (22 wt % W for **POM-SiO$_2$A** and 28 wt % W for **POM-SiO$_2$B**) because of their large molecular weight. EDS confirmed that the high cluster loading was due to POMs incorporated within the macroporous silica frameworks of **POM-SiO$_2$A** and **POM-SiO$_2$B**. TEM analysis of the extracted materials showed a nearly homogeneous distribution of POM clusters throughout the silica walls. This was not the case, however, for a sample of **POM-SiO$_2$B** that was calcined to remove the polystyrene template. For this sample, a bulk tungsten oxide phase separated from the silica framework.

Catalytic Activity. The catalytic activities of **POM-SiO$_2$A** and **POM-SiO$_2$B** were tested for the epoxidation of cyclooctene with anhydrous H_2O_2/*tert*-butyl alcohol at room temperature. An experiment with a pure-silica macroporous sample (**3DOM SiO$_2$**) and a blank experiment with no catalyst were carried out for comparison. The results are listed in Table 1. Both **POM-SiO$_2$A** and **POM-SiO$_2$B** were catalytically active for the epoxidation of cyclooctene. In both cases the selectivity was 100% for the epoxide. In contrast, the **3DOM SiO$_2$** and blank experiments resulted in no cyclooctene conversion. Chemical analysis of the used catalysts showed that there was no leaching of W from the **POM-SiO$_2$** materials during the catalytic tests. IR indicated that the polyoxometalate species in **POM-SiO$_2$A** remained intact following catalytic testing, with retention of the characteristic absorptions. In contrast, the polyoxometalate in **POM-SiO$_2$B** experienced partial degradation with the appearance of new IR bands at 325 and 245 cm^{-1}, in addition to the original bands, which can be attributed to tungsten oxide absorptions. A higher conversion of cyclooctene to the epoxide, based on the substrate, was observed for **POM-SiO$_2$B** (24%) than for **POM-SiO$_2$A** (11%). This difference was more than predicted by the higher POM loading of **POM-SiO$_2$B** (28 wt % W) compared to that of **POM-SiO$_2$A** (22 wt %

(57) van Bekkum, H.; Kloetstra, K. R. *Stud. Surf. Sci. Catal.* **1998**, *117*, 171−182.

W) and indicated that **POM-SiO$_2$B** was the more effective catalyst for this conversion. POM catalysts that more readily decompose by the H_2O_2 co-oxidant are known to be more effective epoxidation catalysts, with epoxidation yields qualitatively correlating with the rate of POM degradation by H_2O_2.[47,58,59] The different yields observed for the **POM-SiO$_2$** catalyzed epoxidations could, therefore, be explained by a greater degradation of the POM species in **POM-SiO$_2$B** during the reaction, which was confirmed by IR of the used catalyst. This result suggests that the γ-$SiW_{10}O_{36}$ POM was stabilized to H_2O_2 degradation by the grafting of organosiloxane units to its surface.

Conclusion

Two methods have been presented for the synthesis of novel three-dimensionally ordered macroporous silica materials functionalized by polyoxometalates. The syntheses utilized the reactivity of lacunary polyoxometalates toward siloxanes to incorporate POMs into 3DOM silica materials by condensation with the silicate framework around polystyrene colloidal crystal templates with or without the presence of bifunctional organosiloxane linkers. The polystyrene was removed from the samples by solvent extraction to produce hybrid macroporous materials containing structurally intact POMs. Alternatively, calcination to remove the polystyrene template led to decomposition of the POMs and aggregation of a bulk tungsten oxide species on the surface of the structure. The direct synthesis procedures allowed for high loadings and a uniform dispersion of POMs throughout the materials. The polyoxometalates remained catalytically active in the hybrid materials, as demonstrated by a test reaction of the epoxidation of cyclooctene with hydrogen peroxide as a co-oxidant.

Acknowledgment. We thank the David and Lucile Packard Foundation, 3M, DuPont, the National Science Foundation (DMR-9701507), and the MRSEC program of the NSF under award number DMR-9809364 for support of this research. C.F.B. acknowledges the Center for Interfacial Engineering for a CIE-NSF graduate fellowship. We thank Sergey Sokolov for assistance with catalytic testing.

CM000830B

(58) Aubry, C.; Chottard, G.; Platzer, N.; Brégeault, J.; Thouvenot, R.; Chauveau, F.; Huet, C.; Ledon, H. *Inorg. Chem.* **1991**, *30*, 4409−4415.

(59) Duncan, D. C.; Chambers, R. C.; Hecht, E.; Hill, C. L. *J. Am. Chem. Soc.* **1995**, *117*, 681−691.